Journal of Mines, Metals and Fuels, *71(12C) : 159-167; 2023. DOI: 10.18311/jmmf/2023/47281*

Print ISSN : 0022-2755

Journal of Mines, Metals and Fuels

Contents available at: *www.informaticsjournals.com/index.php/jmmf*

Radiation Effect on Inclined Peristaltic Couple Stress Fluid Flow in an Asymmetric Horizontal Channel

Avula Sreevallabha Reddy[1], Gullapalli Neeraja[1], B. N. Swetha[2], R. Suresh Babu[1] and P. A. Dinesh[1,2]

[1]*Department of Mathematics, M S Ramaiah Institute of Technology, Bengaluru – 560054, Karnataka, India*

[2]*Department of Mathematics, APJ Abdul Kalam Residential College, Mandya – 571436, Karnataka, India*

Abstract

In the present paper a theoretical investigation on the influence of radiation Impact on the couple stress fluid in an inclined horizontal channel with peristalsis is considered. The velocity, pressure gradient and frictional force are analyzed by utilizing numerical and analytical methods. The numerical outcomes are graphically represented with relevant numerical data in the scientific literature for the non-dimensional physical parameters. The observations show that the trapping fluid is removable and the magnetic field will substantially reduce central line axial velocity.

Keywords: *Heat Generation, Non-Newtonian Power-Law Fluid, Radiation Effect, Shooting Technique, Yield Stress*

1.0 Introduction

Due to growing industrial, medical, and technical applications, the non-Newtonian fluid flow has been obtained significant consideration over the past few years. Different researchers examined various flow models linked to many non-Newtonian fluids, and one among those fluids is the couple stress fluid. The theory of couple stress fluids is developed by Stokes[1] has several applications relevant to biomedical, industrial, and in scientific research. The couple stress fluids which are used in modelling synthetic fluids, animal blood and synovial fluid, fluid crystals, polymer thickened oils. We can observe previous developments in the theory of couple stress fluids in Stokes' book[2] with reference to fundamental fluid flows. Few scientists have recently investigated various couple stress fluid flows on various flow geometries[3-9].

Today, due to their application in physiology and industry, peristaltic flows have gained considerable interest. The peristaltic transport consists of a type of transportation of physiological fluids, driven through a progressive wave of an area of expansion or contraction along the channel/tube. In physiology, it is a significant factor in different circumstances including the motion of food in the tube of digestion, urinal transfer from the kidney to the gallbladder through the ureter, lymph fluid circulation in lymphatic vessels, bile movement into the duodenum from the gallbladder, Male reproductive tract duct spermatozoa efferent, Fallopian tube having a ovum motion, blood flow in the narrow blood vessels, gastrointestinal tract motion of the chyme, intrauterine fluid movement, oesophagus swallowing of food bolus and transporting of cilia. Modern analysis of peristaltic flows of couple stress fluids can be found in the recent literatures[10-14]. Mishra and Rao[15] investigated that the efficiency of peristaltic pumping in an asymmetric channel can be increased for the adverse pressure gradient due to the external magnetic field impact.

Riaz *et al.*[16] has analyzed the study of flow of a peristaltic Carreau fluid in a rectangular compliant channel. Nadeem *et al.*[17] has been presented the peristaltic unsteady flow of Carreau incompressible fluid in eccentric cylinders.

**Author for correspondence*

Shit and Roy[18] investigated the peristaltic transport of physiological fluid in an asymmetric channel under long wave length assumptions and low-Reynolds number flows. Rao and Rao[19] took into consideration the slip velocity at the channel's inclination impact on the peristaltic transport of a pair stress fluid under the influence of an externally supplied magnetic field. Pandey and Chaube[20] analyzed the study of couple stress fluid flow in a peristaltic porous channel under the impact of an external magnetic field along with the travelling waves on the walls of the channel. With the effect of induced magnetic field Nadeem and Akram[21] has presented that the peristaltic transport of a couple stress fluid in an asymmetric channel. Oscillatory Magnetic Hydro Dynamic porous arteriole blood flow in presence of chemical reaction and an external magnetic field was investigated by Misra and Adhikary[22].

In view of thermo therapy in human thermo regulation system, the bio heat transfers in human tissues to contemplate by the biomedical engineers to consider the heat transport models in the human body. Indeed, transfer of heat into human tissues is involving complex procedures including thermal conduction in tissues; thermal transmission because of perfusion through tissue pores of the arterial-venous blood; metabolic heat formation and cellular-emitted electronic radiation on human tissues. Transfer of heat involves in complex procedures like assessing the skin burns, destroying the cancer tissues, blood flow dilution method, paper producing, vasodilation, and environmental radiation. Maheshbabu and Sreenadh[24], discussed the Influence of Hall effects on peristaltic flow of a Carreau fluid in an asymmetric channel. The effects of entropy production and thermal radiation on the peristaltic blood flow of a magneto-micropolar fluid in a tapered channel were explored by Asha *et al.*[25]. The effects of thermal radiation, heat source/sink, and thermal slip on the peristaltic flow of blood in an asymmetric channel have been discussed by Dar[26].

In metal manufacturing processes, maintaining a consistent and controlled flow of metal is essential. Peristaltic couple stress fluid flow analysis could help in optimizing the flow to reduce defects and improve product quality. Peristaltic pumps based on the principles of couple stress fluid flow could be used to accurately extrude molten metal for additive manufacturing processes like 3D printing. In mining operations, the transport of ore as a slurry is common. Understanding the effects of couple stress on the behavior of the ore slurry could help in optimizing transport processes, such as pipeline design and pump selection. Ore beneficiation processes involve the separation of valuable minerals from gangue. Couple stress fluid flow analysis may assist in the design of separation processes by accounting for micro-scale forces affecting particle behavior. In the oil and gas industry, peristaltic pumps designed with couple stress fluid flow principles could be used to transport fuels more efficiently, with less risk of contamination or emulsion formation. Understanding how couple stress affects the flow behavior of fuel in storage tanks and its interaction with tank walls may help in preventing sedimentation, corrosion, and other issues.

Kumar KT *et al.*,[23] analyzed the peristaltic flow of a Jeffrey fluid, incorporating heat and mass transfer phenomena within an inclined asymmetric channel, while accounting for the influence of slip boundary conditions.

Tamara Sh. Ahmed[27] studied the effect of an inclined magnetic field on Carreau fluid peristaltic flow through a porous, tapered asymmetric channel. Yousif R et al.,[28] examined temperature-dependent viscosity effects on MHD blood flow of Ree-Eyring fluid through a porous, inclined asymmetric channel.

According to the above-mentioned applications and studies, and with the acquired knowledge of the author, peristaltic transport of a non-Newtonian fluid in an inclined horizontal channel is not considered. So therefore, an effort has been made to propose a mathematical model of peristaltic transport of couple stress fluid in an inclined asymmetric horizontal channel to study the effect of heat transfer under the influence of an external magnetic field. The analytical and numerical solutions for axial velocity, stream function, and pressure rise per wavelength are found using the long wave length approximations and low Reynolds number. The numerical results were estimated and graphically displayed with MATLAB software. Our theoretical research, therefore, possesses the potential for use in the field of biofluid dynamics.

2.0 Mathematical Modeling and Analysis

Consider the peristaltic transport of blood in an asymmetric inclined horizontal channel with a uniform thickness with the influence of an external magnetic field. Blood is treated as an electrically conducting couple stress fluid and an incompressible viscous fluid. The Cartesian coordinates are (x, y) for a point, X is taken along the direction of the peristaltic wave, and Y in the direction

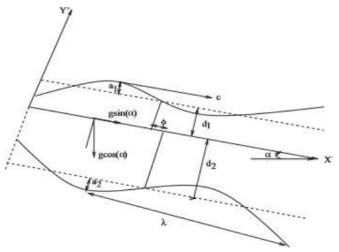


Figure 1. Sketch of the proposed co-ordinate system.

perpendicular to the average location of the corresponding blood vessel. Let $\overline{Y} = \overline{h}_1$ and $\overline{Y} = \overline{h}_2$ show respectively the lower and the upper wall of the asymmetric channel[30]. The flow medium is taken into account to be propagated with sinusoidal wave train with a wave speed c along the channel wall (Figure 1).

$$\overline{h}_1(\overline{X},\overline{t}) = d_1 + a_1 \cos\left[\frac{2\pi}{\lambda}(\overline{X} - c\overline{t})\right], \tag{1}$$

$$\overline{h}_2(\overline{X},\overline{t}) = -d_2 - a_2 \cos\left[\frac{2\pi}{\lambda}(\overline{X} - c\overline{t}) + \phi\right], \tag{2}$$

where, d_1 and d_2 are the average height of the upper and lower channel wall from the centre of the channel, a_1 and a_2 are the waves' amplitudes of the channel walls, λ represents wavelength, $\phi(0 \le \phi \le \pi)$ the phase gap between the two wall trains. The flow of fluid in the channel occurs through a uniform external magnetic transverse constant force field B_0, and induced magnetic field is ignored due to small Reynolds number.

The momentum and heat transfer equations are considered in the for an incompressible couple stress fluid, in the absence of body couples are [29]

$$\frac{\partial \overline{U}}{\partial X} + \frac{\partial \overline{V}}{\partial Y} = 0, \tag{3}$$

$$\rho\left(\frac{\partial \overline{U}}{\partial \overline{t}} + \overline{U}\frac{\partial \overline{U}}{\partial \overline{X}} + \overline{V}\frac{\partial \overline{U}}{\partial \overline{Y}}\right) = -\frac{\partial \overline{P}}{\partial \overline{X}} + \overline{\mu}\left(\frac{\partial^2 \overline{U}}{\partial \overline{X}^2} + \frac{\partial^2 \overline{U}}{\partial \overline{Y}^2}\right) - \overline{\eta}\left(\frac{\partial^4 \overline{U}}{\partial \overline{X}^4} + 2\frac{\partial^4 \overline{U}}{\partial \overline{X}^2 \partial \overline{Y}^2} + \frac{\partial^4 \overline{U}}{\partial \overline{Y}^4}\right) - \sigma B_0^2 \overline{U} + \rho g \beta_T (\overline{T} - \overline{T}_0)\sin\alpha, \tag{4}$$

$$\rho\left(\frac{\partial \overline{V}}{\partial \overline{t}} + \overline{U}\frac{\partial \overline{V}}{\partial \overline{X}} + \overline{V}\frac{\partial \overline{V}}{\partial \overline{Y}}\right) = -\frac{\partial \overline{P}}{\partial \overline{Y}} + \overline{\mu}\left(\frac{\partial^2 \overline{V}}{\partial \overline{X}^2} + \frac{\partial^2 \overline{V}}{\partial \overline{Y}^2}\right) - \overline{\eta}\left(\frac{\partial^4 \overline{V}}{\partial \overline{X}^4} + 2\frac{\partial^4 \overline{V}}{\partial \overline{X}^2 \partial \overline{Y}^2} + \frac{\partial^4 \overline{V}}{\partial \overline{Y}^4}\right) - \rho g \beta_T (\overline{T} - \overline{T}_0)\cos\alpha, \tag{5}$$

$$\rho C_p\left(\frac{\partial \overline{T}}{\partial \overline{t}} + \overline{U}\frac{\partial \overline{T}}{\partial \overline{X}} + \overline{V}\frac{\partial \overline{T}}{\partial \overline{Y}}\right) = K^*\left(\frac{\partial^2 \overline{T}}{\partial \overline{X}^2} + \frac{\partial^2 \overline{T}}{\partial \overline{Y}^2}\right) + Q_0 - \frac{\partial \overline{q}_r}{\partial \overline{Y}}. \tag{6}$$

The relative heat flux is calculated with the approximation of Rosseland

$$\overline{q}_r = -\frac{4\sigma^*}{3\alpha_r}\frac{\partial \overline{T}^4}{\partial \overline{Y}}. \tag{7}$$

The temperature differences within the flow are assumed in such a way that $\overline{T}^4$ can be expressed as a linear function of the temperature $\overline{T}$. This could be achieved by expanding $\overline{T}^4$ in a Taylor's series about $\overline{T}_0$, which is assumed to be independent of $\overline{Y}$, and neglecting powers higher than one of $\overline{T}$. Thus, we get

$$\overline{T}^4 = 4\overline{T}_0^3\overline{T} - 3\overline{T}_0^4. \tag{8}$$

Then the heat transfer equation takes the form

$$\frac{\partial \overline{T}}{\partial \overline{t}} = \frac{\overline{K}}{pc_p}\frac{\partial^2 \overline{T}}{\partial \overline{Y}^2} + \frac{16\sigma^*\overline{T}_0^3}{3pc_p\alpha_r}\frac{\partial^2 \overline{T}}{\partial \overline{Y}^2}.$$

Considering the wave frame (x,y) that moves away from the fixed frame with a velocity c from the fixed frame (X, Y), we use the transformation

$$\overline{x} = \overline{X} - c\overline{t}, \overline{y} = \overline{Y}, \ \overline{u} = \overline{U} - c, \ \overline{v} = \overline{V},$$

$$\overline{p}(\overline{x},\overline{y}) = \overline{P}(\overline{X},\overline{Y},\overline{t}), \ T(x,y) = \overline{T}(\overline{X},\overline{Y},\overline{t}) \tag{9}$$

In the velocity elements $(\overline{u},\overline{v})$ and $(\overline{U},\overline{V})$ of the frame and the fixed frame, $\overline{P}$ and $\overline{p}$ are for wave pressure along with the fixed frame of referral accordingly, and T represents temperature in the reference wave and fixed frame.

We introduce the following dimensionless parameters:

$$\overline{x} = \frac{x}{\lambda}, \overline{y} = \frac{y}{d_1}, h_1 = \frac{H_1}{a_1}, h_2 = \frac{H_2}{d_1}, \overline{u} = \frac{u}{c},$$
$$\overline{v} = \frac{v}{c}, \ \overline{v} = \frac{v}{c}, p = \frac{d_1^2\overline{p}}{\lambda\eta c}, \overline{t} = \frac{ct}{\lambda}, \overline{v} = \frac{\lambda v}{d_1 c}, p = \frac{d_1^2}{\lambda\eta c}\overline{p}$$

$$\delta = \frac{d_1}{\lambda}, d = \frac{d_2}{d_1}, a = \frac{a_1}{d_1}, b = \frac{a_2}{d_1}, \theta = \frac{T - \overline{T}_0}{\overline{T}_1 - \overline{T}_0}. \tag{10}$$

where, μ represents the fluid viscosity, η represents the constant connected with couple stress fluid, the fluid pressure represents by p, ρ represents the fluid density, σ represents the electrical conductivity, α represents

the inclination of the channel, g represents the acceleration due to gravity, δ denotes the dimensionless wave number, $\overline{T}_0$ and $\overline{T}_1$ are the temperatures at the lower and upper wall of channel, respectively.

$$\delta\frac{\partial u}{\partial x}+\frac{\partial v}{\partial y}=0, \tag{11}$$

$$\mathrm{Re}\,\delta\left((u+1)\frac{\partial u}{\partial x}+v\frac{\partial v}{\partial y}\right)=-\frac{\partial p}{\partial x}+\left(\delta^2\frac{\partial^2 u}{\partial x^2}+\frac{\partial^2 u}{\partial y^2}\right)-\frac{1}{\gamma^2}\left(\delta^4\frac{\partial^4 u}{\partial x^4}+\frac{\partial^4 u}{\partial y^4}\right)-M^2(u+1)+Gr\,\theta\sin\alpha, \tag{12}$$

$$\mathrm{Re}\,\delta^3\left((u+1)\frac{\partial v}{\partial x}+v\frac{\partial v}{\partial y}\right)=-\frac{\partial p}{\partial y}+\left(\delta^3\frac{\partial^2 v}{\partial x^2}+\delta\frac{\partial^2 v}{\partial y^2}\right)-\frac{1}{\gamma^2}\left(\delta^5\frac{\partial^4 v}{\partial x^4}+2\delta^3\frac{\partial^4 v}{\partial x^2\partial y^2}+\delta\frac{\partial^4 v}{\partial y^4}\right)-Gr\,\delta\cos\alpha, \tag{13}$$

$$\mathrm{Re}\,\mathrm{Pr}\,\delta\left((u+1)\frac{\partial\theta}{\partial x}+v\frac{\partial\theta}{\partial y}\right)=\delta^2\frac{\partial^2\theta}{\partial x^2}+(1+N_r)\frac{\partial^2\theta}{\partial y^2}+\beta \tag{14}$$

$$\begin{aligned}&\mathrm{Re}=\frac{pcd_1}{\mu},\ M=\sqrt{\frac{\sigma}{\mu}}B_0d_1,\ \gamma=\sqrt{\frac{\mu}{\eta}}d_1,\\&G_r=\frac{pgd_1^2\beta_T(T-\overline{T}_0)}{\mu c},\ \mathrm{Pr}=\frac{\mu c_p}{k^*},\\&\beta=\frac{Q_0d_1^2}{k^*(\overline{T}_1-\overline{T}_0)},\ Nr=\frac{16\sigma^*\overline{T}_0^3}{3\alpha_rK}\end{aligned} \tag{15}$$

Re stands for Reynolds number, M for Hartmann number, γ represents couple stress parameter, Gr represents Grashof number of local temperature, *Pr* is Prandtl number, θ is the dimensionless temperature, β is heat generation parameter, N_r is thermal radiation parameter.

The dimensionless velocity components (u,v) in terms of stream function ψ are related by the subsequent relations:

$$u=\frac{\partial\psi}{\partial y},\qquad v=-\delta\frac{\partial\psi}{\partial x} \tag{16}$$

Using the long wave length approximation (δ≤1) and low Reynolds number, the equations (12)-(14) takes the form

$$0=-\frac{\partial p}{\partial x}+\frac{\partial^3\psi}{\partial y^3}-\frac{1}{\gamma^2}\frac{\partial^5\psi}{\partial y^5}-M^2\left(\frac{\partial\psi}{\partial y}+1\right)+Gr\theta\sin\alpha, \tag{17}$$

$$0=\frac{\partial p}{\partial y}, \tag{18}$$

$$0=(1+N_r)\frac{\partial^2\theta}{\partial y^2}+\beta. \tag{19}$$

Eliminating pressure p from the equations (17) and (18), we obtain

$$\frac{\partial^6\psi}{\partial y^6}-\gamma^2\frac{\partial^4\psi}{\partial y^4}+M^2\gamma^2\frac{\partial^2\psi}{\partial y^2}-Gr\gamma^2\sin\alpha\frac{\partial\theta}{\partial y}=0. \tag{20}$$

The non-dimensional BC's are

$$\psi=\frac{F}{2},\ \frac{\partial\psi}{\partial y}=-1,\ \frac{\partial^3\psi}{\partial y^3}=0,\ \theta=0\ \text{at}\ y=h_1, \tag{21}$$

$$\psi=-\frac{F}{2},\ \frac{\partial\psi}{\partial y}=-1,\ \frac{\partial^3\psi}{\partial y^3}=0,\ \theta=1\ \text{at}\ y=h_2. \tag{22}$$

where, $h_1=1+a\cos(2\pi x)$

and $h_2(x)=-d-b\cos(2\pi x+\phi)$ represent the dimensionless form of the peristaltic walls such that a, b, d and φ satisfy the relation

$$a^2+b^2+2ab\cos\phi\le(1+d)^2.$$

The dimensionless mean flow rate Θ is given by

$$\Theta=F+1+d, \tag{23}$$

where, $$F=\int_{h_1}^{h_2}\frac{\partial\psi}{\partial y}dy=\psi(h_2(x))-\psi(h_1(x)). \tag{24}$$

Solving the equations (19) and (20) using the boundary conditions (21) and (22) the expressions for temperature θ and stream function ψ are obtained as follows

$$\theta=A_1y^2+A_2y+A_3 \tag{25}$$

$$\begin{aligned}\Psi=&D_1y^3+D_2y^2+D_3y+D_4+D_5\cosh(\lambda y)\\&+D_6\sinh(\lambda y)+\phi(y)\end{aligned} \tag{26}$$

where, $A_1=\frac{-\beta}{2(1+N_r)};A_2=\frac{C_1}{1+N_r};A_2=\frac{C_1}{1+N_r};;$

$$\gamma^2=a_1;C_1=\frac{\beta}{2}(h_1+h_2)+\frac{1+N_r}{h_1-h_2};\ a_3=G_ra_1;$$

$$C_2 = \frac{1+N_r}{h_2-h_1}h_2 - \frac{\beta h_1 h_2}{2};\ a_2 = \sqrt{a_1^2 - 4a_1M^2};$$

$$\lambda_1^2 = \frac{a_1+a_2}{2};\ \lambda_2^2 = \frac{a_1-a_2}{2};\ a_4 = 2A_1a_3;$$

$$a_5 = a_3A_2;$$

$$a_6 = \frac{a_4}{6a_1M^2};\ a_7 = \frac{a_5}{2a_1M^2}$$

$$\phi(y) = \frac{G_r\, Sin\alpha}{6M^4}\left(M^2+1\right)\left(2A_1\, y^3 + 3A_2y^2\right). \quad (27)$$

The boundary conditions are applied on the equation (26) and the resulting equations are solved for D_1 to D_6 numerically using MATLAB.

The pressure rise per wave length is numerically calculated using the formula

$$\Delta P = \int_0^1 \frac{dp}{dx}dx. \quad (28)$$

3.0 Results and Discussion

"Computations are carried for the study of velocity, temperature, pressure gradient, wave length pressure rise for various parameters like Gr, Nr , M, β and γ and also fixing other parameters constants for understanding the characteristics change for a couple stress fluid in an inclined peristaltic flow of horizontal channel using MATLAB software. Figures 2-7 shows the axial velocity u profile at the channel height for different values of Grashof number *Gr*, Couple stress parameter γ , Heat generation parameter β and Hartmann number M, thermal radiation parameter Nr and the inclination of the channel . It has been found from the Figure that maximum velocity is always close at the centre of the channel, and in almost all cases velocity profiles are parabolic. This illustration shows that the velocity increases up to a certain point which we call it a point of inflection after it gradually decreases. That is the height of the channel the velocity reduces with a rise in the Grashof number Gr values. At the lower wall of the channel, the buoyancy force is more so it increases the velocity." As the as the fluid moves towards the upper rises the influence of buoyancy decreases and hence the velocity of the fluid decreases. Figure 3 provides an idea of the velocity variation occurring as the external magnetic field intensity change, i.e. with the change in the amount of Hartmann Number M. We observe here that the velocity decreases with the Hartmann Number M increase on the central channel line. This result is like the actual situation, when the magnetic field is applied to the fluid, it creates a force transversal to the direction of application of magnetic field. This body force is termed as Lorentz force that appears to slow down fluid velocity. Figure 8 and Figure 9 shows changes in the distribution of temperature in the peristaltic fluid movement in the basic situation studied during the study. The plots in Figures 8, 9 provide some important details about the transfer of heat into the fluid mass. Figures 8, 9 show that with β heat source/sink parameter value, temperature increases, whereas the various plots shown in Figure 9 shows a different pattern when *Nr* changes its value in the thermal radiation parameter. This illustration indicates the thermal radiation has an important impact on the temperature profile. This argument can be made by looking at the temperature profile and comparing it with graphs that have nonzero thermal radiation parameter values. A significant observation can be made here that thermal boundary thickness decreases as thermal radiation is increased. We prefer to predict that radiation is sufficiently high at high temperatures; the curves of temperature distribution are nearly coincidental. The plots shown in Figure 9 show that the phase difference significantly affects the distribution of temperature and thermal boundary layers decrease with an increasing phase difference. Furthermore, the original point is slowly transferred to the central channel region with an increasing difference in phases.

3.1 Pumping Characteristics

In the analysis of the transportation of the physiological fluid, pumping properties are the main aspects. The pumping idea is determined by the change in the average flux of time with a pressure difference over one wavelength. It is well known that the instantaneous difference in stress between 2 stations of 1 wavelength apart is constant when the flow in the wave setting is constant. The axial pressure gradient varies over a wavelength is presented for similar interest physical parameters Figures 9-13.

From Figure 10, we can observe that the flow can't move easily through region , the narrower part of the channel. Thus, an extra gradient of pressure is needed for normal flux likewise fluid can easily move over

the broad section of the channel, that is, in and) due to lower pressure gradients. Figure 10 demonstrates the variation of Hartmann number's axial pressure gradient. We note that the axial pressure gradient amplitude also rises as Hartmann values rises. It indicates that if a strong magnetic field is subjected to flow, the flow must pass through a higher-pressure gradient. This finding implies that a suitable magnetic field strength can be used to regulate fluid pressures. This phenomenon is useful to avoid excessive bleeding during critical operations. Figure 11 shows a difference in the channel inclination of the axial pressure gradient.

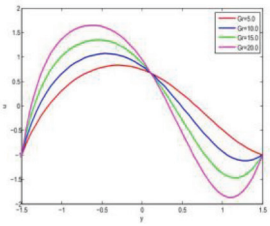


Figure 2. Velocity profile for various values of Gr.

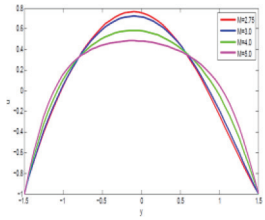


Figure 3. Velocity profile for various values of M.

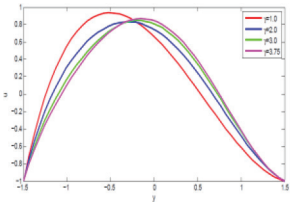


Figure 4. Velocity profiles for various values of γ.

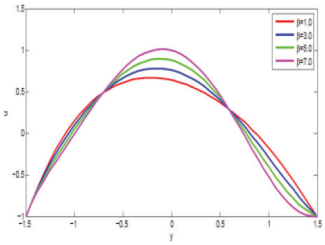


Figure 5. Velocity profiles for various values of β.

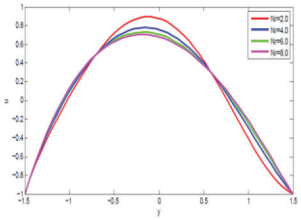


Figure 6. Velocity profiles for various values of Nr.

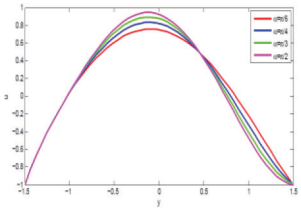


Figure 7. Velocity profiles for various values of α.

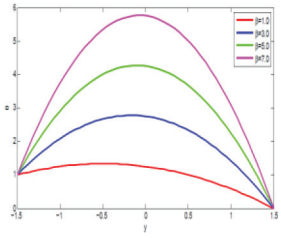


Figure 8. Distribution of temperature for various values of β.

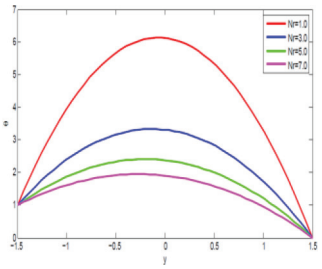


Figure 9. Distribution of temperature for various values of Nr.

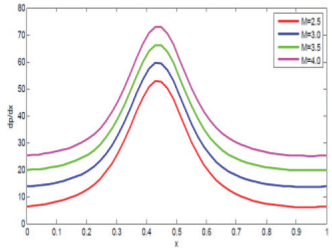


Figure 10. Pressure gradient for different M.

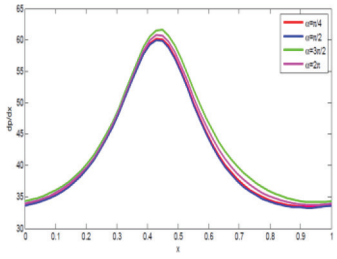


Figure 11. Pressure gradient variation for different α.

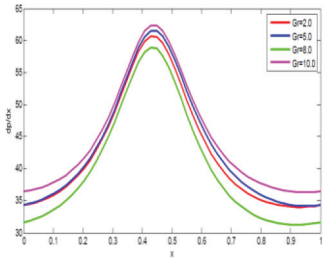


Figure 12. Pressure gradient for different Gr values.

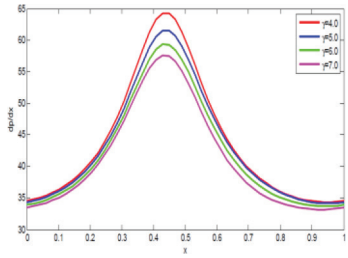


Figure 13. Pressure gradient for different γ values.

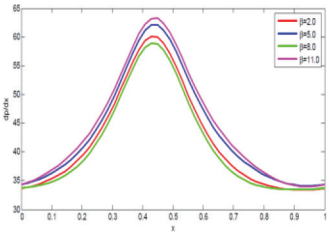


Figure 14. Pressure gradient for different β values.

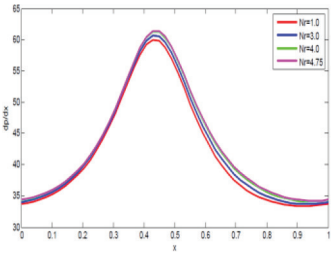


Figure 15. Pressure gradient for different Nr values.

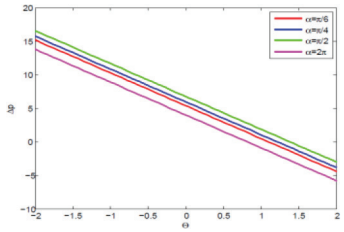


Figure 16. Wave length pressure for different values of α.

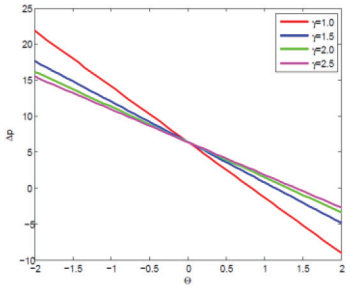


Figure 17. Wave length pressure for various values of γ.

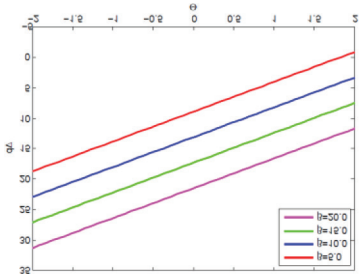


Figure 18. Wave length pressure for different β values.

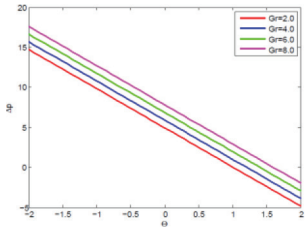


Figure 19. Wave length pressure for different Gr values.

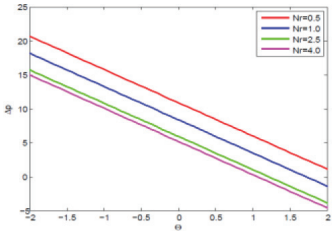


Figure 20. Wave length pressure rise for different Nr values.

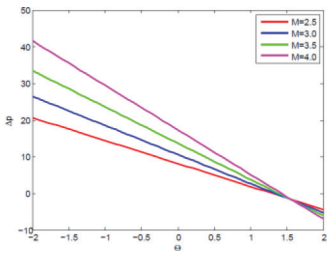


Figure 21. Wave length pressure for different values of M.

This demonstrates that when the channel inclination increases, the pressure gradient increases. Hence, the same fluid volume for the channel inclination allows more pressure to be transferred.

4.0 Conclusions

The research reveals the important fact that wave amplitude, couple stress effect, heat source parameter β, angle of inclination α, and Froude number Fr are significantly influenced by the velocity. The important conclusion of this research is that meantime the flux reversal is enhanced by an increase in pressure in the free pump case; the flux reversal can be decreased by increasing the stress effect of the couple. If the pressure increase ΔP is negative, the stress impact for couples produces flow resistance whereby the velocity is decreased, but the flow is increased by the stress impact for couples in the event of pumping free ΔP=0. Based on this observation one can conclude that pumping and pressure can be increased by increasing both amplitude and couple stress parameters.

The increased number of Hartmann raises the pressure gradient. It shows that if the flow area is applied by a strong magnetic field, a greater-pressure gradient is demanded to get the flow through. This outcome shows the fluid pressure would be regulated using sufficient magnetic field strength. This is beneficial in surgery and the treatment of great hemorrhage.

5.0 References

1. Stokes VK. Couple stresses in fluids. Phys Fluids. 1966; 9(9):1709-15. https://doi.org/10.1063/1.1761925.
2. Stokes VK. Theories of fluids with microstructure. Springer, USA: New York; 1984. https://link.springer.com/book/10.1007/978-3-642-82351-0
3. Devakar M, Iyengar TKV. Run up flow of a couple stress fluid between parallel plates. Nonlinear Anal: Model Control. 2010; 15(1):29-37. https://www.journals.vu.lt/nonlinear-analysis/article/view/14362
4. Devakar M, Iyengar TKV. Stokes problems for an incompressible couple stress fluid. Nonlinear Anal: Model Control. 2008; 1(2):181-90. https://doi.org/10.15388/NA.2008.13.2.14578
5. Hayat T, Mustafa M, Iqbal Z, Alsaedi A. Stagnation point flow of couple stress fluid with melting heat transfer. Appl Math Mech. 2013; 34(2):167-76. https://doi.org/10.1007/s10483-013-1661-9
6. Akbar NS, Nadeem S. Intestinal flow of a couple stress nanofluid in arteries. IEEE Trans. Nanobioscience. 2013; 12(4):332-39.
7. Srinivasacharya D, Srinivasacharyulu N, Odelu O. Flow and heat transfer of couple stress fluid in a porous channel with expanding and contracting walls. Int Commun Heat Mass Transf. 2009; 36(2): 180-5. https://doi.org/10.1016/j.icheatmasstransfer. 2008.10.005
8. Muthuraj R, Srinivas S, Immaculate DL. Heat and mass transfer effects on MHD fully developed flow of a couple stress fluid in a vertical channel with viscous dissipation and oscillating wall temperature. Int J Appl Math. 2013; 9(7): 95-117. https://doi.org/10.1002/htj.21040
9. Srivastava VP, Saxena M. A two-fluid model of non Newtonian blood flow induced by peristaltic waves. Rheologica Acta. 1995; 34(4):406-14. https://doi.org/10.1007/BF00367155
10. Pandey SK, Chaube MK. Study of wall properties on peristaltic transport of a couple stress fluid. Meccanica. 2011; 46(6):1319-30. https://doi.org/10.1007/s11012-010-9387-8
11. Ali N, Hayat T. Peristaltic flow of a micropolar fluid in an asymmetric channel. Comput Math Appl. 2008; 55(4):589-608. https://doi.org/10.1007/s11012-010-9387-8
12. Rani PN, Sarojamma G. Peristaltic transport of a Casson fluid in an asymmetric channel. Australas Phys Eng Sci Med. 2007; 27(2):49-59. https://doi.org/10.1007/BF03178376
13. Hayat T, Afsar A, Ali N. Peristaltic transport of a Johnson-Segalman fluid in an asymmetric channel. Math Comput Model. 2008; 47(3-4):380-400. https://doi.org/10.1016/j.mcm.2007.04.012
14. Hayat T, Javed M. Exact solution to peristaltic transport of power-law fluid in asymmetric channel with compliant walls. Appl Math Mech. 2010; 31(10):1231-40. https://doi.org/10.1007/s10483-010-1356-7
15. Mishra M, Rao AR. Peristaltic transport of a Newtonian fluid in an asymmetric channel. Z Angew Math Phys. 2003; 54(3):532-50.
16. Riaz A, Ellahi R, Nadeem S. Peristaltic transport of a Carreau fluid in a compliant rectangular duct. Alex Eng J. 2014; 53:475-484. https://doi.org/10.1016/j.aej.2014.01.005
17. Nadeem S, Riaz A, Ellahi R, Akbar NS. Series solution of unsteady peristaltic flow of a Carreau fluid in eccentric cyl-

inders. Ain Shams Eng J. 2014; 5(1):293-304. https://doi.org/10.1016/j.asej.2013.09.005
18. Shit GC, Roy M. EYKN Effect of induced magnetic field on peristaltic flow of a micropolar fluid in an asymmetric channel. Int J Numer Method Biomed Eng. 2010; 26 (11):1380-403. https://doi.org/10.48550/arXiv.1007.092
19. Rao TR, Rao DRVP. Peristaltic flow of a couple stress fluid through a porous medium in a channel at low Reynolds number. Int J Appl Math Mech. 2012; 8 (3):97-116.
20. Pandey SK, Chaube MK. Effect of magnetic field on peristaltic transport of couple stress fluids through a porous medium. J Biol Syst. 2011; 19(2):251-62. https://doi.org/10.1142/S0218339011003890
21. Nadeem S, Akram S. Peristaltic flow of a Couple stress fluid under the effect of induced magnetic field in an asymmetric channel. Arch Appl Mech. 2011; 81:97-109. https://doi.org/10.1007/s00419-009-0397-8
22. Misra JC, Adhikary SD. MHD oscillatory channel flow, heat and mass transfer in a physiological fluid in presence of chemical reaction. Alex En. J. 2015. https://doi.org/10.1016/j.aej.2015.10.005
23. Kumar KT, Kumar PM, Srilatha P, Fareeduddin M. Peristaltic flow of Jeffery fluid with heat and mass transfer through an inclined asymmetric tapered channel under an influence of slip boundary conditions. J Xidian Univ. 2020; 14(5).
24. Maheshbabu N, Sreenadh S. Influence of Hall effects on peristaltic flow of a Carreau fluid in an asymmetric channel. J Math Comput Sci. 2020.
25. Asha SK, Deepa CK. Entropy generation for peristaltic blood flow of a magneto-micropolar fluid with thermal radiation in a tapered asymmetric channel. Results Eng. 2019; 3:100024. https://doi.org/10.1016/j.rineng.2019.100024
26. Dar AA. Effect of thermal radiation, temperature jump and inclined magnetic field on the peristaltic transport of blood flow in an asymmetric channel with variable viscosity and heat absorption/generation. Iran J Sci Technol - Trans Mech. 2020; 7. https://doi.org/10.1007/s40997-020-00349-6
27. Tamara Sh. Ahmed. Effect of inclined magnetic field on peristaltic flow of Carreau Fluid through porous medium in an inclined tapered asymmetric channel. Al-Mustansiriyah J Sci. 2019; 29(3):94. https://doi.org/10.23851/mjs.v29i3.641
28. Yousif R, Ali HA. Temperature-dependent viscosity effect on the peristaltic transport of (MHD) blood flow Ree-Eyring fluid through porous medium in an inclined asymmetric channel. Al-Qadisiyah J Pure Sci. 2020; 25(3):16-34. https://doi.org/10.29350/qjps.2012.17.3.1118
29. Shit GC, Roy M. Hydromagnetic effect of inclined peristaltic flow of a couple stress fluid. Alex Eng J. 2014; 53:949-58. https://doi.org/10.1016/j.aej.2014.07.007
30. Ramesh K, Devkar M. Effects of heat and mass transfer on the peristaltic transport of MHD couple stress fluid through porous medium in a vertical channel. J Fluids Eng. 2015:ID 163832. https://doi.org/10.1155/2015/163832